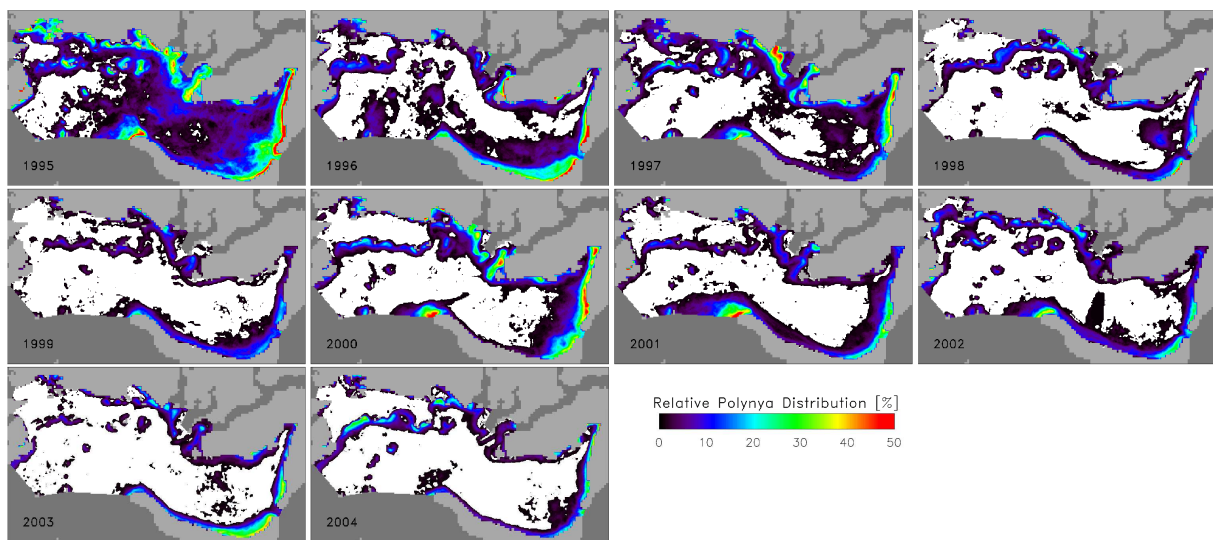


## 8 Get polynya area time-series (3.2.8)

### 8.1. Kara Sea polynya area

The PSSM has been applied to SSMI data of DMSP-platforms f10, f13 and f15 (see section 1.2) to obtain the polynya area time-series of the Kara Sea for 1995-2007. Figure 19 shows the mean wintertime (Jan.-Apr.) polynya distribution in the Kara Sea for the period 1995-2004. Figure 20 shows the respective time series of the total Kara Sea polynya area for the period 1995-2004. This data is not restricted to Jan.-Apr. but starts when the entire Kara Sea is ice covered and/or the Kara gate is closed with ice, and ends when melting conditions seem to hamper a meaningful estimation of the polynya distribution using the PSSM (typically end of April / middle of May). Part of this figure served as the base for the comparison with models (section 7).



**Figure 19:** Relative polynya distribution as observed with the PSSM in the Kara Sea for Jan.-Apr. of the period 1995-2004. Given is the number of the used twice-daily overpasses during which open water or thin ice has been classified in the respective grid cell (of size 5 km x 5 km), e.g. light blue denotes areas where in about 20 % of the used data a polynya occurred. White areas mark a probability for the occurrence of a polynya of less than 0.5 %. Land is flagged light grey, areas with missing data or data flagged as not belonging to the region of interest are given in dark grey.

In order to extend the polynya area time series backwards, i.e. to the period when 85 GHz data were not available, the daily mean polynya area of months January to April of 1996-2003 has been compared to the mean daily sea ice area of the Kara Sea derived from NASA-Team algorithm sea ice concentration data of a certain selected ice concentration range of the same period. The resulting linear relationship between normalized sea ice area and total polynya area (Figure 21 a) has been used subsequently to derive a time-series of the total Kara Sea polynya area for the period 1978/79 until 2003/04 (Figure 21 b), Kern, 2008).

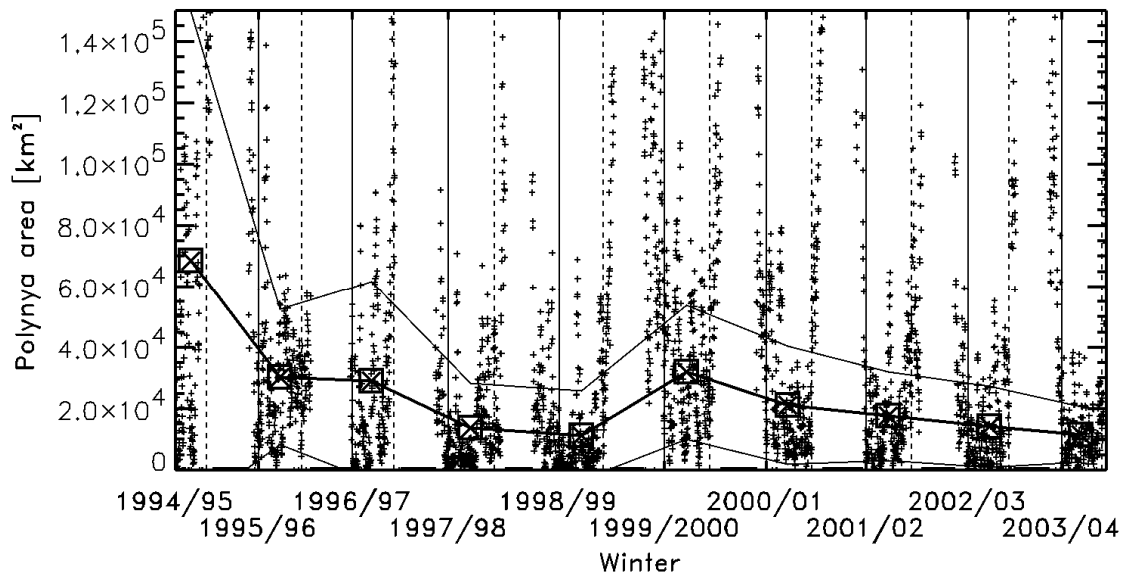


**Figure 20:** Time series of the twice daily thin-ice area in the Kara Sea obtained with the PSSM for 1995 – 2004; squares connected by the thick solid line denote the average winter (Dec.-Apr.) polynya area, the thin lines denote plus or minus one standard deviation.

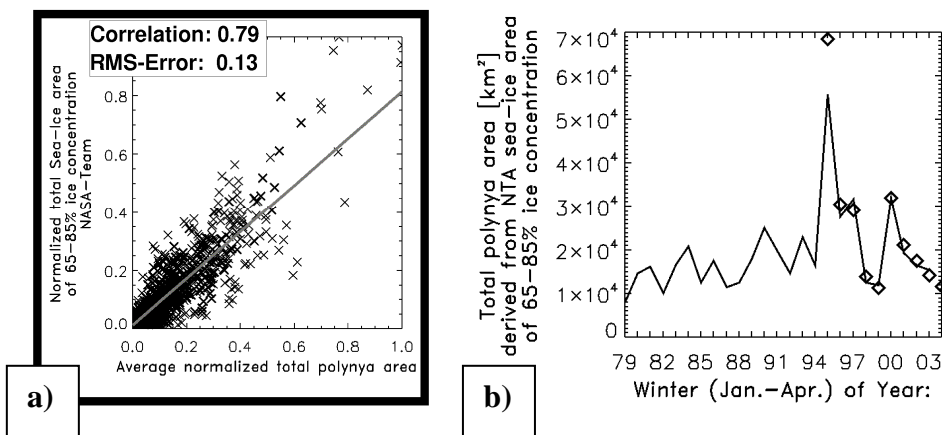
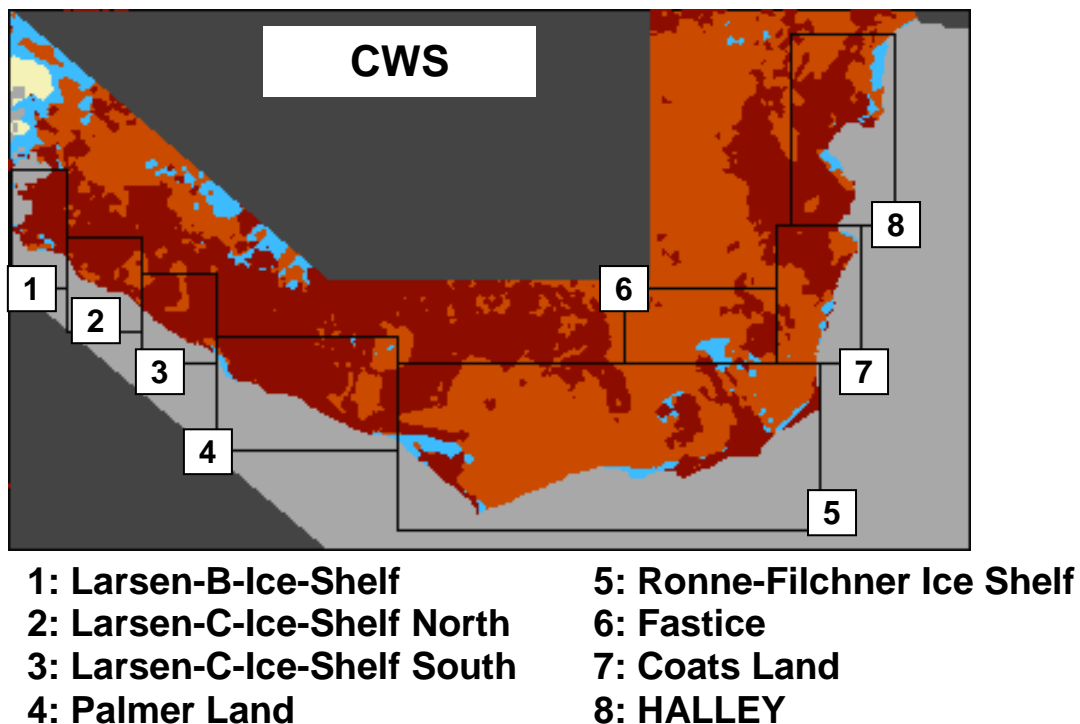


**Figure 21:** a) Scatterplot of the normalized mean daily sea ice area of the ice concentration range 65-85% and the normalized mean daily PSSM-based polynya area of Jan.-Apr. 1996-2003. b) Time series of the wintertime total polynya area of the Kara Sea as obtained with the mentioned linear relationship (solid line) and with the PSSM (diamonds).

## 8.2 Polynya area: Central Weddell Sea (CWS)

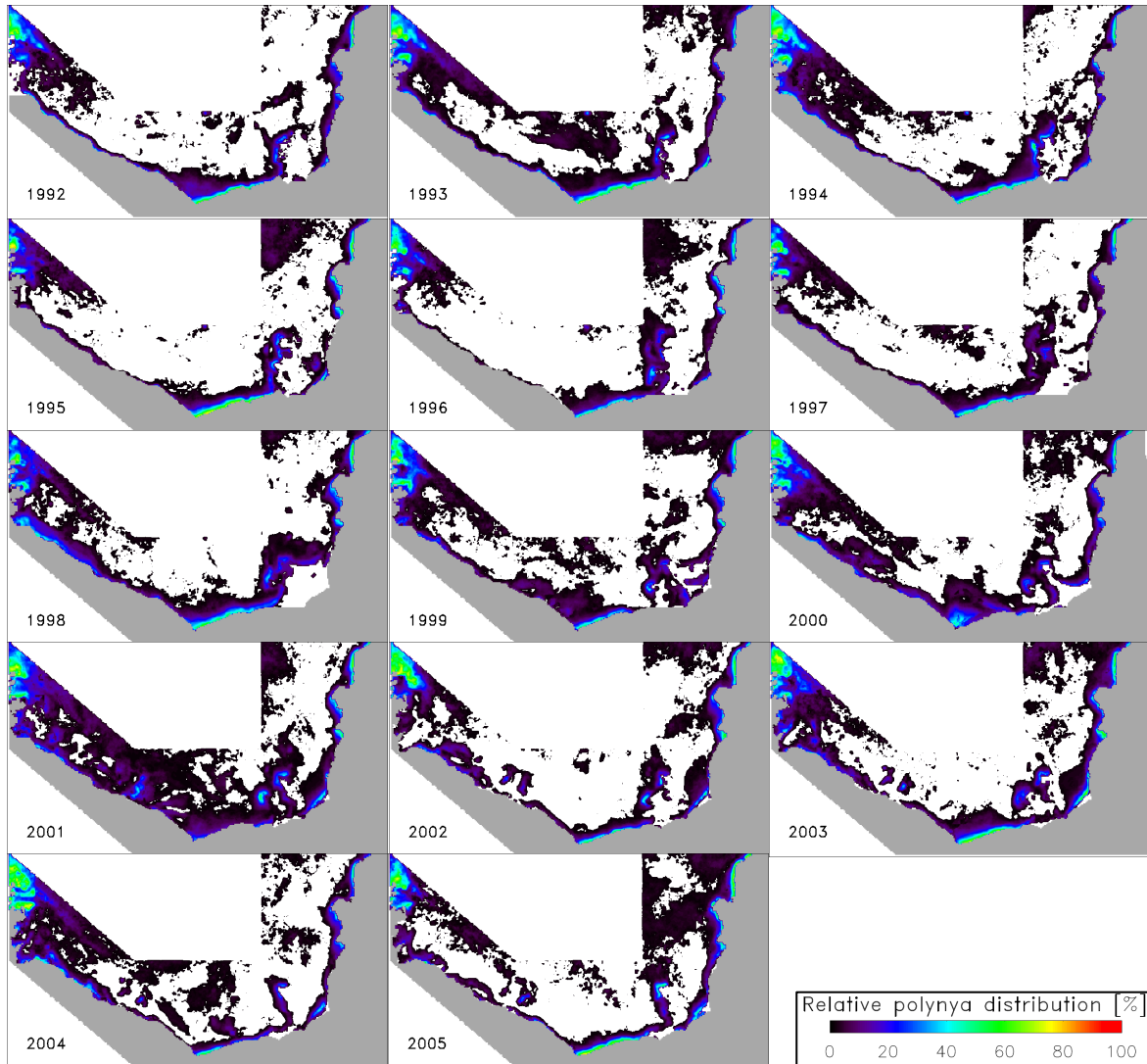
The PSSM has been applied to DMSP-f10, -f13, and -f15 SSM/I swath data covering all regions given in Figure 2 for the period 1992-2006 (region WRS: until today, see [http://www.ifm.zmaw.de/~wwwrs/RS\\_RossSeaPolynyaMaps.html](http://www.ifm.zmaw.de/~wwwrs/RS_RossSeaPolynyaMaps.html)). SSM/I data of May.-Sep. are used, i.e. when the sea ice extent is large enough to allow the consideration of near-coastal open water areas as a polynya. Only for regions CWS and WRS the application period includes April also. The mentioned post-processing (flagging of temporally stable ice, see Section 2) is carried out. Using the quality measures mentioned in Section 2 a supervised list of the obtained maps of the polynya distribution is made for every region for every year.

In the following, the entire polynya area time series will be given separately for each region, starting with a sample map, which shows the region in detail and which gives the sub-regions used to calculate a) the polynya area, and b) the associated ice and salt production (see Section 9). This further yet not mentioned division into sub-regions has been regarded necessary because of two reasons. First, although at least two maps are used to exclude those areas from the PSSM analysis, which might bias the retrieval of the polynya area (see Section 2), the regions that are used up (Figure 2) are considered too large for a physically meaningful determination of the polynya area time series. The subsequently introduced sub-regions are much smaller and therefore more suitable to obtain reasonable polynya area time series. Secondly, these sub-regions are used to ease the comparison with earlier work regarding the polynya area and associated ice and brine production (e.g. Massom et al., 1998; Van Woert, 1999; Renfrew et al., 2002; Marsland et al., 2004; Flocco, 2007; Martin et al., 2007)



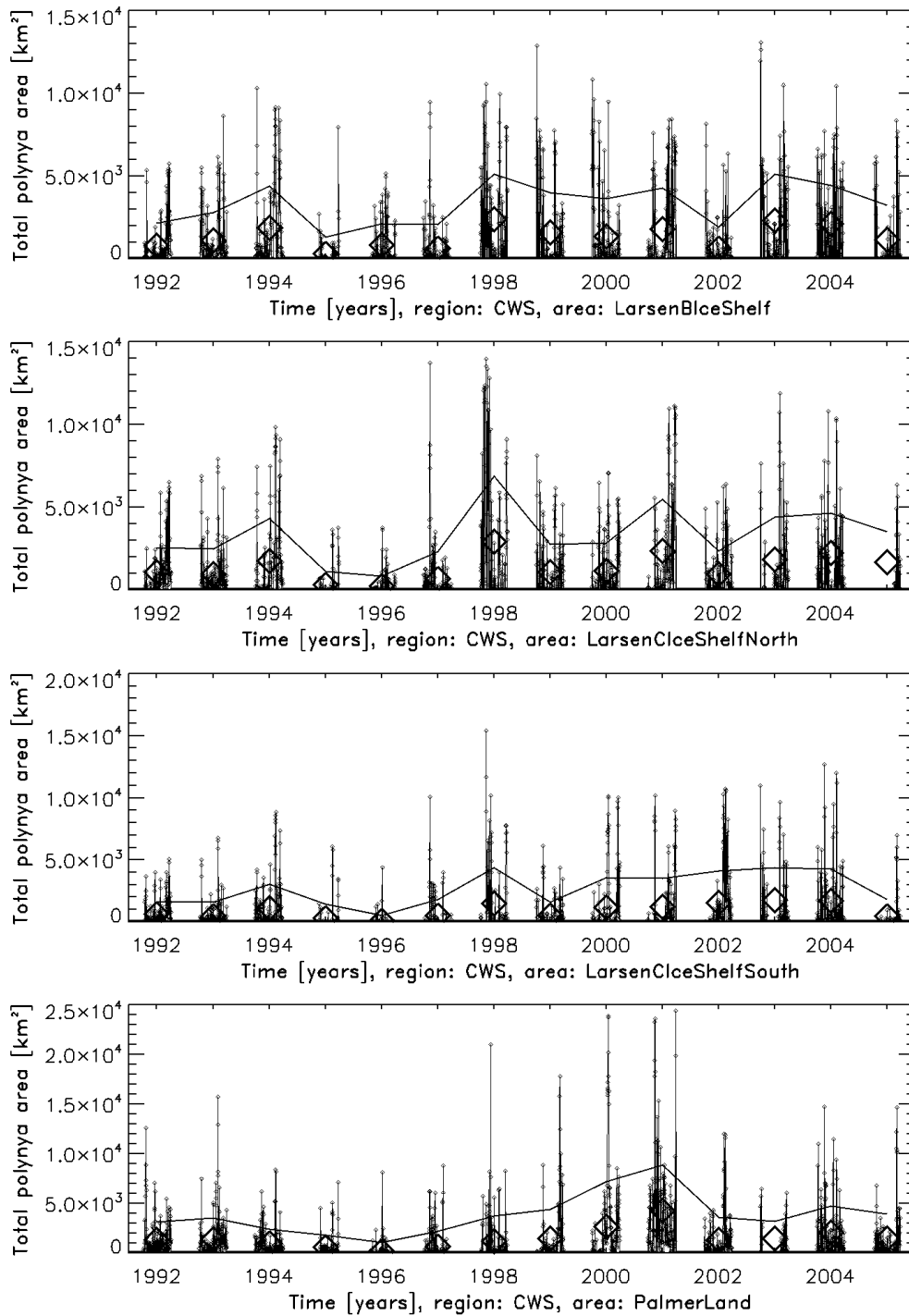
**Figure 22:** Zoom of region CWS (compare Figure 3) showing the sub-regions selected to derive the polynya area time series and to calculate the ice and salt production time series.

Figure 22 shows a sample polynya distribution of the region CWS together with the sub-regions used. Note that the upper left part of the region, which is often already beyond the ice edge is not included in the further analysis of the polynya area and/or ice production. Sub-region 6 is simply an extension of sub-region 5 in an area of the Weddell Sea, which is quite regularly subject to a solid fast ice coverage along which polynyas are generated. This becomes more clear in Figure 23. The coastline of all sub-regions except 6 (Fastice) is a mixture of ice shelf and the Antarctic landmass coast, the latter dominating in Palmer Land (4) and Coats Land (7), and the former dominating in sub-regions 1-3 and 5.



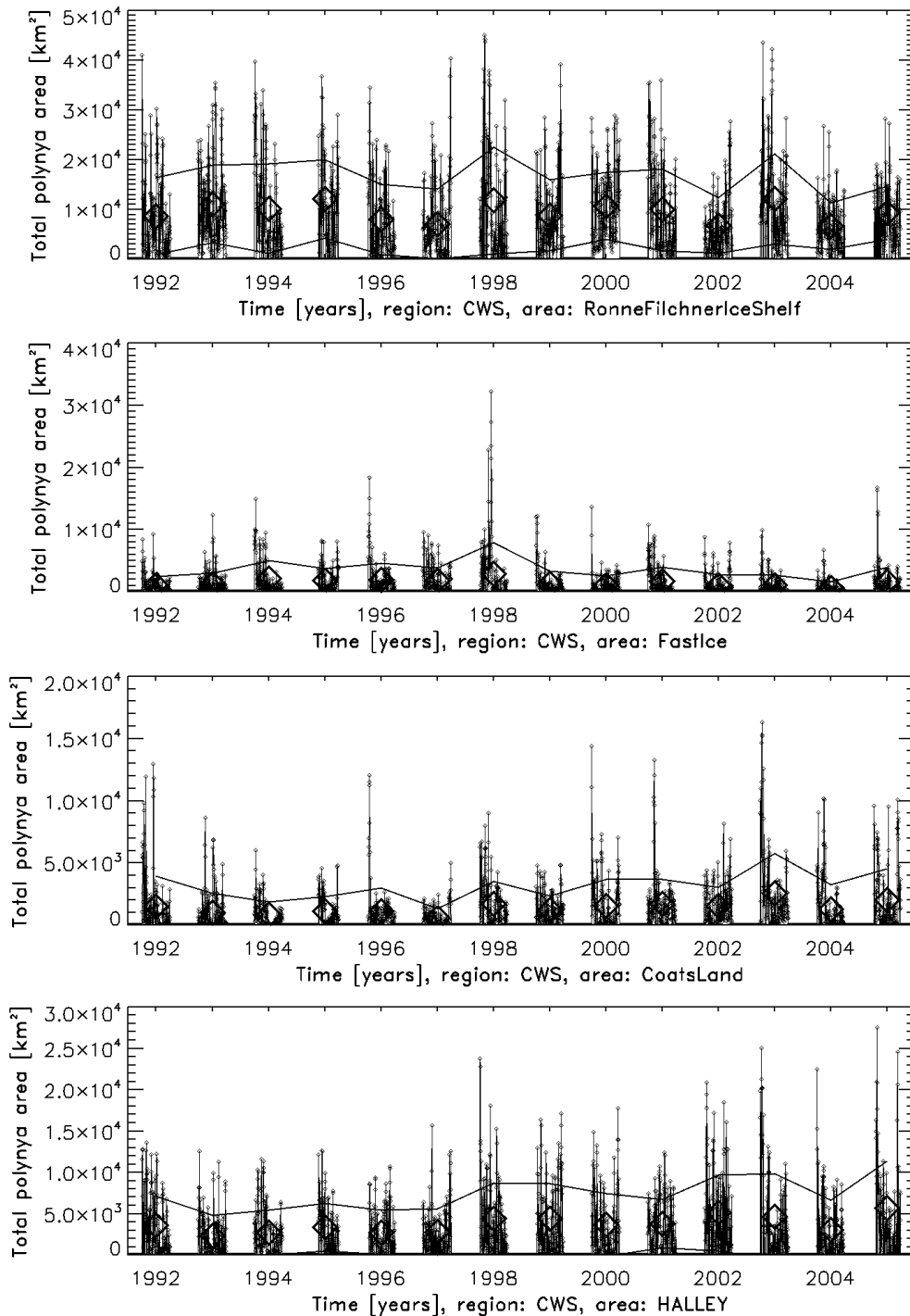
**Figure 23:** *Relative polynya distribution of region CWS for the period 1992-2005. The distribution gives the probability of the occurrence of thin ice or open water in the respective grid cell for the period Apr.-Sep. of each year. A value of 40 (light blue) means that in 40 % of the included PSSM maps a polynya was found. White regions denote missing and/or flagged data or grid cells where the probability is below 0.5 %. The continent and shelf ice area are denoted grey.*

Figure 23 shows, similar to Figure 19, the relative polynya distribution in the region CWS for Apr.-Sep. for the period 1992-2005. A value of 40 % (light blue) means that in 40 % of the used PSSM maps a polynya (i.e. thin ice or open water) has been found for the respective grid cell. These maps reveal quite some variability in the probability of the polynya occurrence. For example, polynya probability along the Ronne-Filchner Ice Shelf (sub-region 5, Figure 22) takes much smaller values in the winters 1999, 2000, and 2001 compared to most other years. This is the sub-region with the highest wintertime polynya probability peaking 75 % in 1995 and 2005. Polynyas along the temporally varying fast ice coverage in the southeastern Weddell Sea are nicely depicted and can also occur with a probability as high as 40 % (2001). Other hotspots of polynya development are in the northernmost part of sub-region 7 (Coats Land, e.g. 2003) and in sub-region HALLEY (sub-region 8), which shows its highest polynya probability in 2005.



**Figure 24:** Total polynya area of sub-regions 1-4 of region CWS (see Figure 22) for Apr.-Sep. 1992-2005. Small symbols connected by thin lines denote sub-daily value; large diamonds denote the average total polynya area; the solid line above and below the large symbols gives the envelope of one standard deviation to these average values. Note that the scale at the y-axis varies.

Figure 24 shows the total polynya area of the eight sub-regions of region CWS (Figure 22) for Apr.-Sep. 1992-2005. Values derived from single PSSM maps are displayed together with the mean (large diamonds, average of the total polynya area taken from all single PSSM maps of the respective sub-region for Apr.-Sep.) total polynya area and its standard deviation (thick solid line). The total polynya area of a sub-region is the sum of all grid cells defined as



**Figure 24, continued.**

Open water or thin ice within that sub-region multiplied by the average area occupied by one grid cell, which is approximately 25 km<sup>2</sup>.

These time series indicate that the Ronne-Filcher Ice Shelf polynya has by far the largest (average) area of around 10 000 km<sup>2</sup>, followed in size by the sub-region HALLEY, where the mean total polynya extent has been around 4000 km<sup>2</sup>. For this sub-region the mean total polynya area seems to have increased during the winters of the shown period. However, when restricting the calculation of the mean polynya area to months June/July/Aug. this trend vanishes (see Figures 25 and 26). Table 2 at the end of Section 8 summarizes the mean total polynya area of all sub-regions using all single PSSM polynya distribution maps and just

those of June/July/Aug., respectively. Minimum mean total polynya areas occurred in sub-region 5 in the years 1997, 2002, and 2004. Note that the polynya distribution maps of these years (Figure 23) do not differ substantially from those of the other years, though. However, in case of the sub-region 4 (Palmer Land), which reveals an elevated mean total polynya area in 2000 and particularly in 2001, peaking 5000 km<sup>2</sup>, the polynya distribution maps differ. These elevated area values have been caused probably by the presence of a large iceberg off the coast of Palmer Land downwind of which a polynya formed (probabilities exceed 30 % in 2001, see Figure 23).

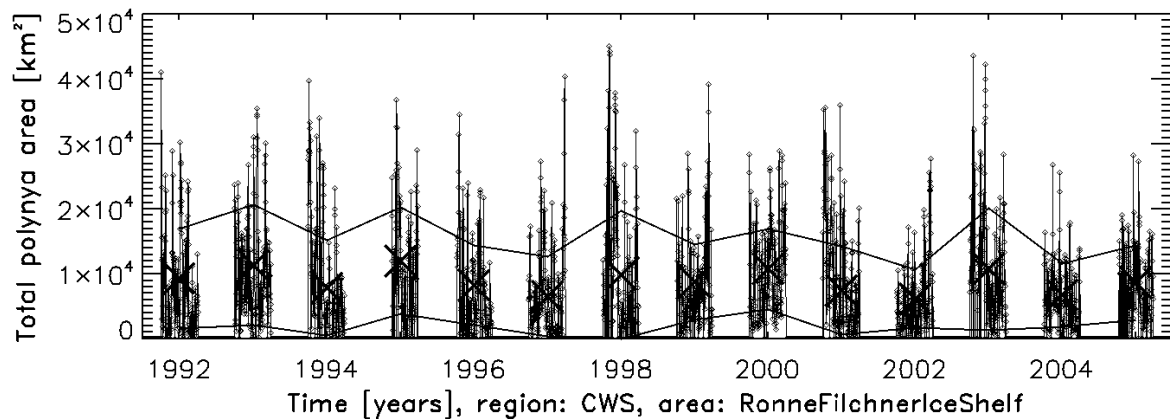


**Figure 25:** Same as Figure 24 but restricted to June-Aug., sub-region 5 (Ronne-Filchner Ice Shelf) and using crosses instead of diamonds to denote the mean total polynya area.

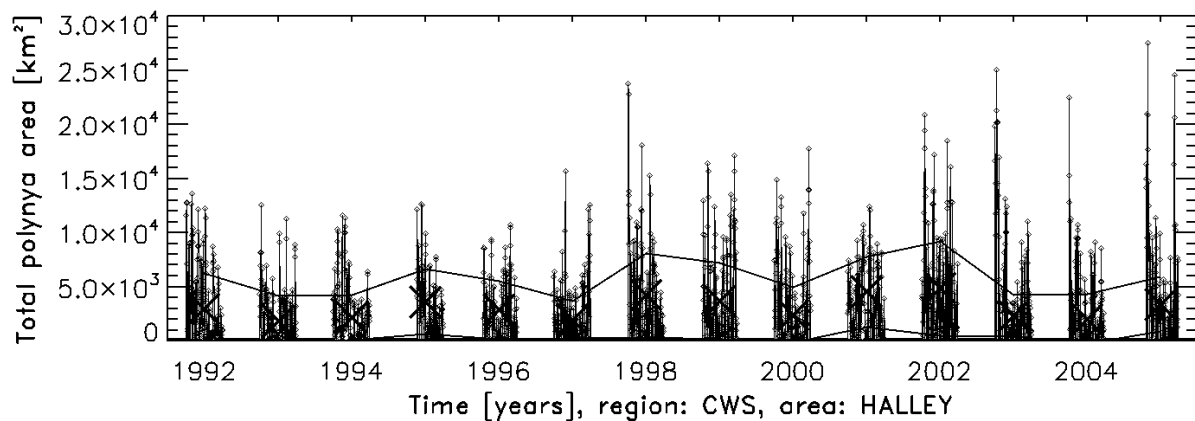
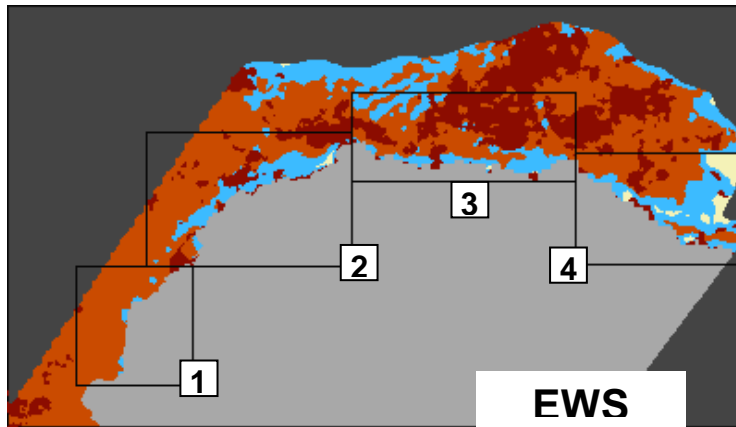


**Figure 26:** Same as Figure 25 but for sub-region HALLEY.

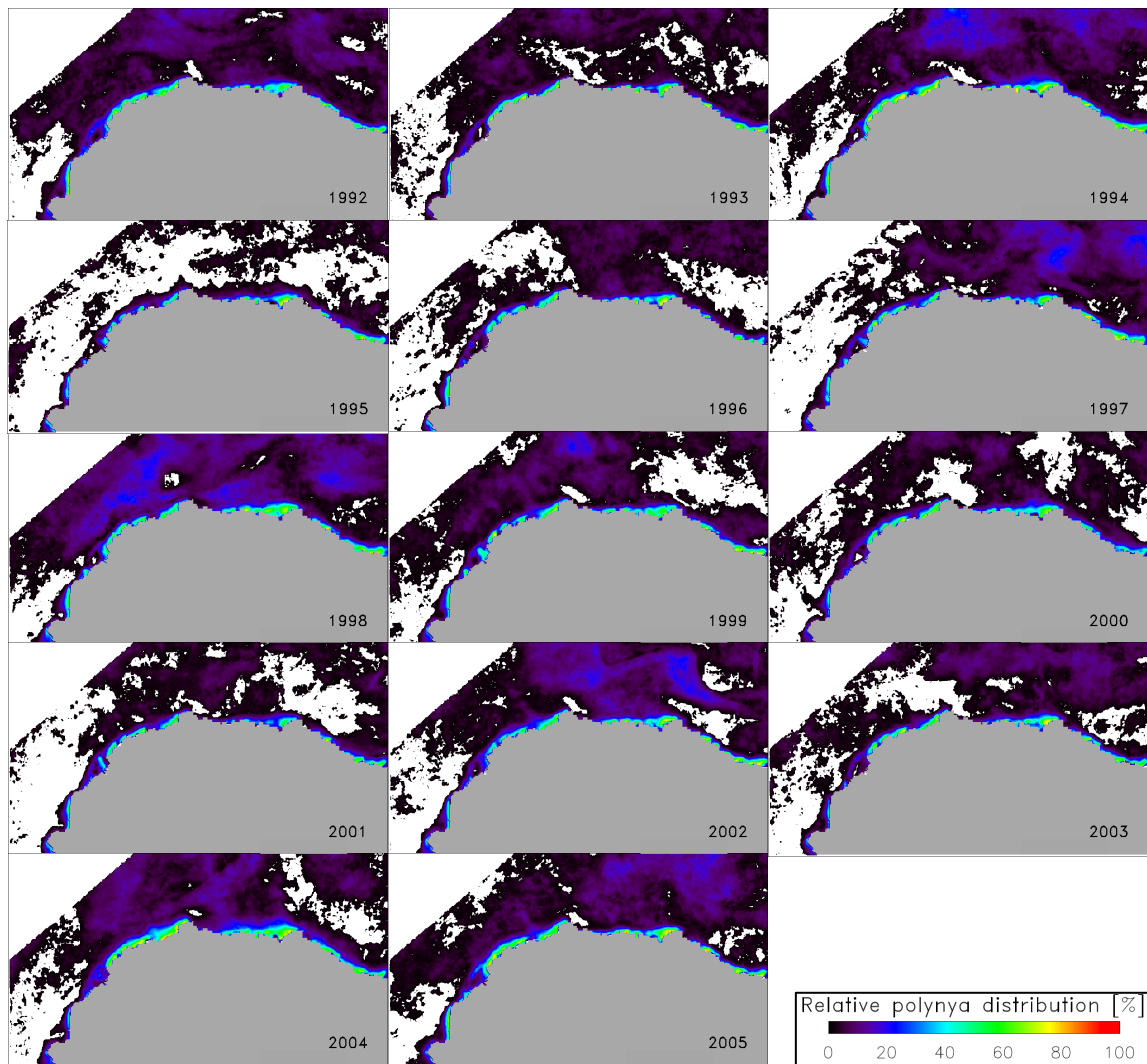
### 8.3 Polynya area: Eastern Weddell Sea (EWS)

Figure 27 shows a sample polynya distribution of the region EWS together with the four sub-regions used. Sub-region 1 overlaps with sub-region 8 of region CWS (see Figure 22). Common for all these sub-regions is that the coastline again comprises a mixture of ice shelf and the coastline of the Antarctic continent / islands. Figure 28 displays the relative wintertime (May to Sep.) polynya distribution of the entire region EWS for the period 1992-2005. This Figure shows that basically the entire coastline of the region EWS is subject to the formation of polynyas with probabilities peaking at 80 %, i.e. on 80 % of the included PSSM-based polynya distribution maps are polynya was find for the respective grid cell. Years with



- 1: Riiser-Larsen Ice Shelf
- 2: NEUMAYER
- 3: Fimbul Ice Shelf
- 4: Riiser-Larsen Sea West

**Figure 27:** Zoom of region EWS – similar to Figure 22.



**Figure 28:** Relative polynya distribution of region EWS for the period 1992-2005 (see caption of Figure 23 for details).

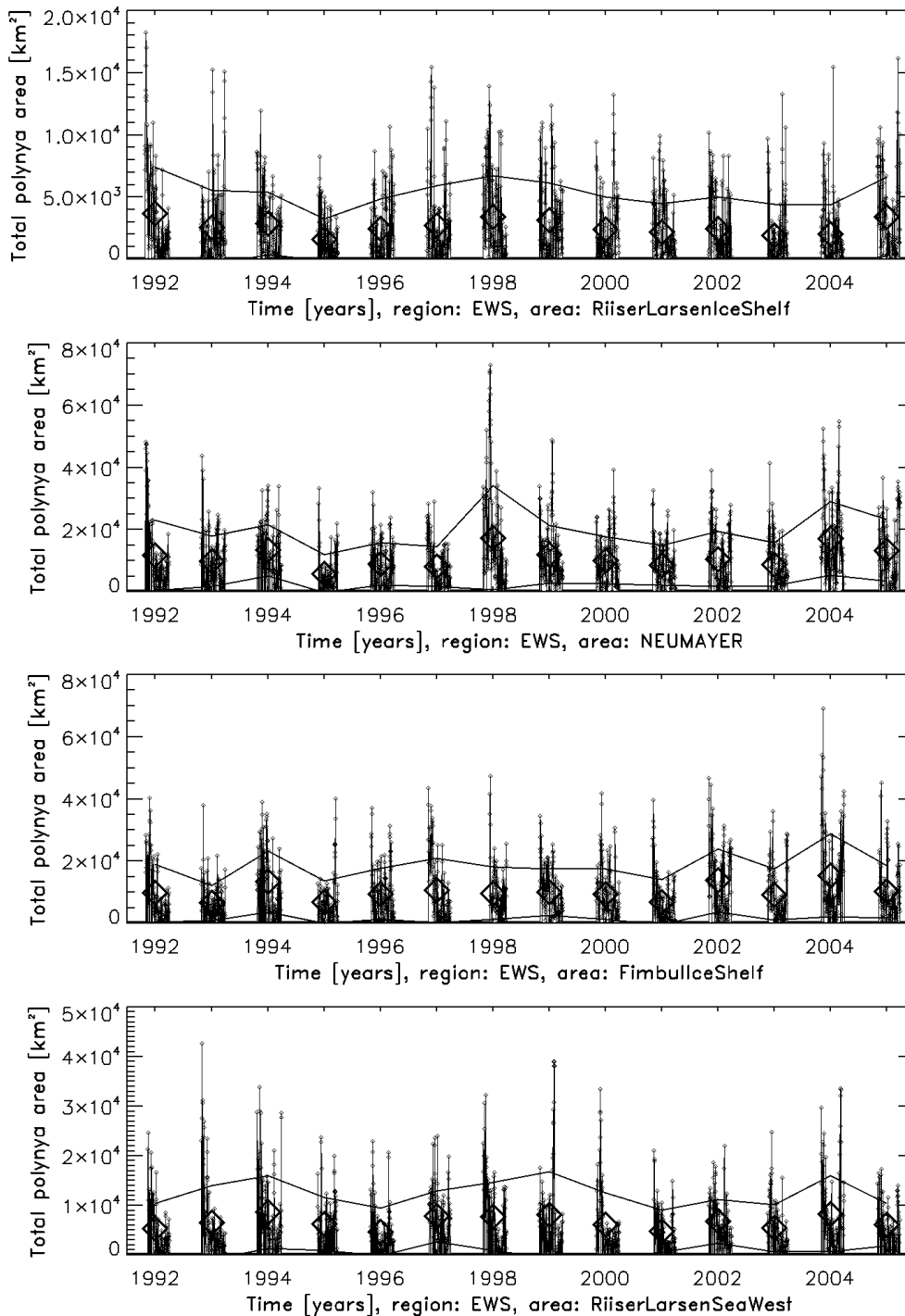


**Figure 29:** Total polynya area of sub-regions 1-4 of region EWS (see Figure 27) for May–Sep. 1992-2005 (see caption of Figure 24 for further details).

a rather low polynya activity along the coast (e.g. 1993, 2001) interchange with years of high polynya probability (e.g. 1994, 1998, 2004).

In addition a substantial relative polynya distribution can be observed well off the coast with peak values of about 30 % in 1994, 1997, 1998, 1999, 2002. In 1994, 1998, and 2002 these areas of enhanced polynya variability occur approximately at the Greenwich meridian (the line separating sub-regions 2 and 3 in Figure 27). They can probably be attributed to a weak Weddell Sea polynya, which occasionally develops in the vicinity of Maud Rise (e.g. Carsey, 1980; Lindsay et al., 2004). Those areas of enhanced polynya probability, which are located

north of sub-region 4 in the eastern part of the region EWS in 1994, 1997, and 2002, are most likely caused by a temporal retreat of the ice edge during the early freezing season. If this retreat happens fast enough the masking procedure described in Section 2 is not able to completely remove the influence of the retreating ice edge from the PSSM analysis. Consequently the PSSM detects the open water and thin ice areas along the ice edge (see Figure 27, sub-region 4). However, the Weddell Polynya as well as the regions of enhanced polynya probability due to a retreating ice edge are outside the sub-regions defined in Figure 27 and therefore do not influence the time series of the total polynya area shown in Figure 29 for all four sub-regions. See the text associated with Figure 25 for a description about how the shown mean total polynya areas have been computed. Sub-regions 2 and 3 reveal the largest mean total polynya area of around 10 000 km<sup>2</sup> (see Table 2), followed by sub-region 4 (around 6000 km<sup>2</sup>) and sub-region 1, which overlaps with sub-region HALLEY of region EWS (around 3000 km<sup>2</sup>). None of the sub-regions show a trend in the average total polynya area. The most interesting years in terms of the polynya area are 1998 and 2004, when this average total polynya area of sub-region 2 peaks at a value of about 16 500 km<sup>2</sup>. Figure 28 reveals that these peak values are partly caused by a substantial fraction of polynyas that have developed off the coast. Figure 30 reveals the cause for this event, showing the sea-ice concentration as calculated with the ARTIST Sea Ice (ASI) concentration algorithm (Kaleschke et al., 2001) from SSM/I 85 GHz data for 6 days in May/June 1998 (images a) to f) together with two selected PSSM maps of the region EWS (images g) and h).

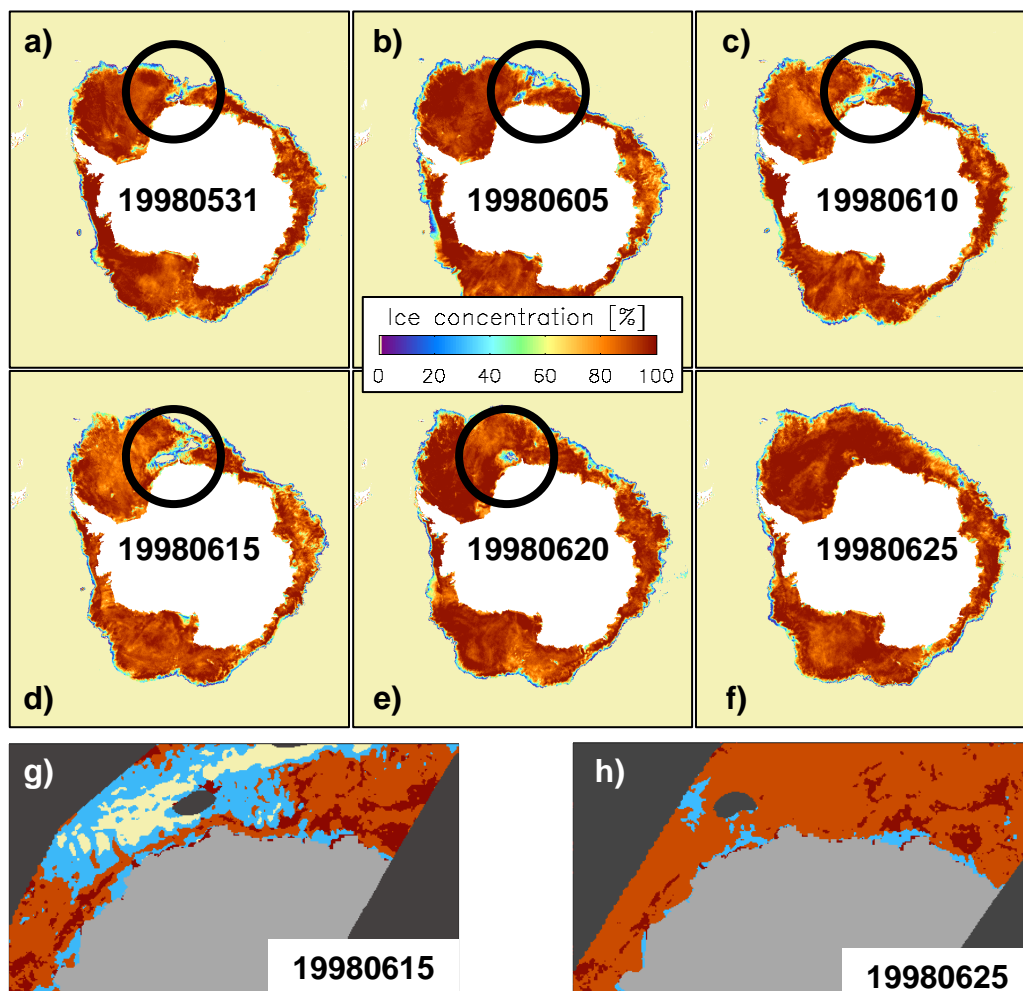


**Figure 30:** Images a) to f): ASI algorithm sea ice concentration of the Southern Ocean for the given dates. Black circles denote the embayment / developing polynya. Images g) and h): PSSM maps of the polynya distribution in region EWS for June 15 and 25, 1998, respectively.

During freeze-up an embayment of open water (see black circles in Figure 30) extended approximately along the Greenwich Meridian southward and further southwestward towards the central Weddell Sea. Although the sea-ice edge advanced further northward this embayment remained open and subsequently formed a vast polynya, which took about 3-4 weeks to close.

#### 8.4 Polynya area: Western Indian Ocean Sector (WIS)

Figure 31 displays a sample PSSM map of region WIS together with the four selected sub-regions. The coastline in this region comprises less shelf ice but more the coastline of the Antarctic landmass, particularly in regions 3 and 4. Note that PSSM-results of this region could also be subject to the influence of ice edge retreat and advance, and also of an embayment in the sea ice cover, which is rather typical for the coast off Enderby Land (sub-region 4), an embayment which is also known as Cosmonaut Sea Polynya when the embayment is shed off the ice edge and becomes a polynya (Comiso and Gordon, 1987, 1996; Geddes and Moore, 2007).

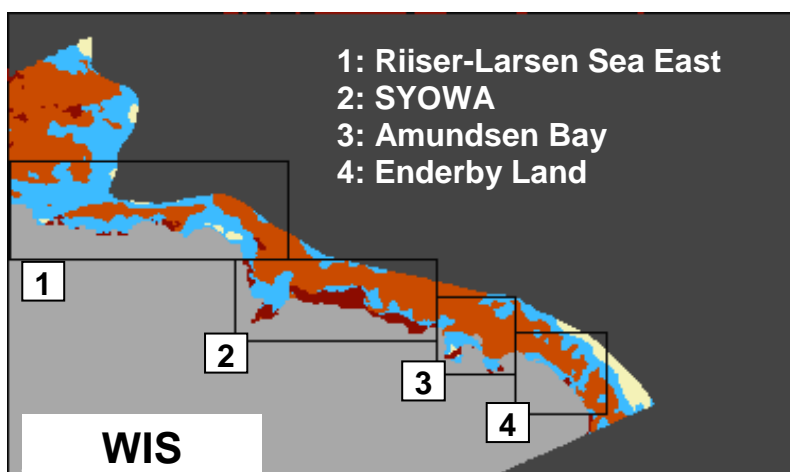


**Figure 31:** Zoom of region WIS – similar to Figure 22.

Figure 32 shows the relative polynya distribution for the region WIS for May-Sep. for the period 1992-2005 as based on PSSM-maps. These maps reveal high inter-annual variability in the polynya probability. This variability is associated a) with the speed of ice-cover development during the early freezing season, b) the variability of the ice edge advance and retreat, and c) the development of embayments in the ice cover off the coast of Enderby Land (sub-region 4 in Figure 31). The bays in sub-regions 2 and 3 (e.g. Lützow-Holm Bay with the Japanese Station Syowa, see red arrow in Figure 32) become typically filled with fast ice every winter, which extends a few ten kilometers northward. Consequently, highest polynya probabilities are found at the border of this belt of fast ice, off Enderby Land (sub-region 4) and in sub-region 1, which overlaps with sub-region 4 of region EWS. Peak values are around 50 to 60 %; only off Enderby Land peak values of 75 to 80 % can be observed (1997, 2001). In fact the polynyas along the fast ice seem to play a minor role compared to the coastal polynyas in sub-regions 1 and 4.

Figure 32 reveals – similar to Figure 28 – quite large areas well off the coast with elevated polynya distribution values peaking at least at 30 % if not at 50 % (1994, 2003). Further up, Figure 30 showed one example of how the ice cover around Antarctica could develop during June. Evidently during June 1998, the sea ice edge stayed quite close to the coast and only at

the end of the month a major northward advance of the ice edge could be observed. The respective polynya distribution map given in Figure 32 reveals in fact a band-like feature of elevated (peaks at about 20 %) polynya probability values stretching at some distance to the coast along the coastline (see red ellipse). A similar feature can be observed almost every year. This effect is most pronounced in years 1996 and 2002. During these years the ice edge

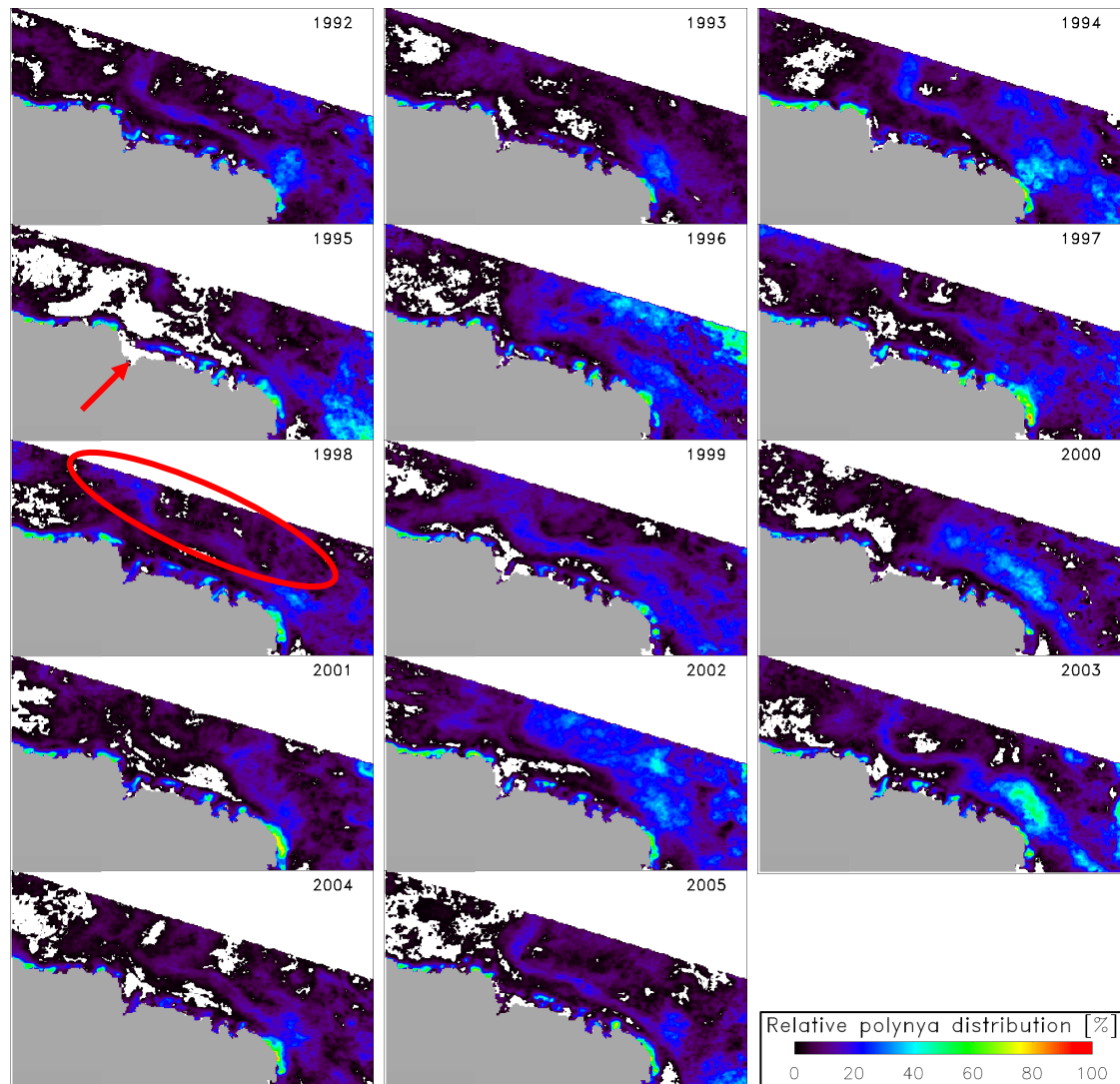
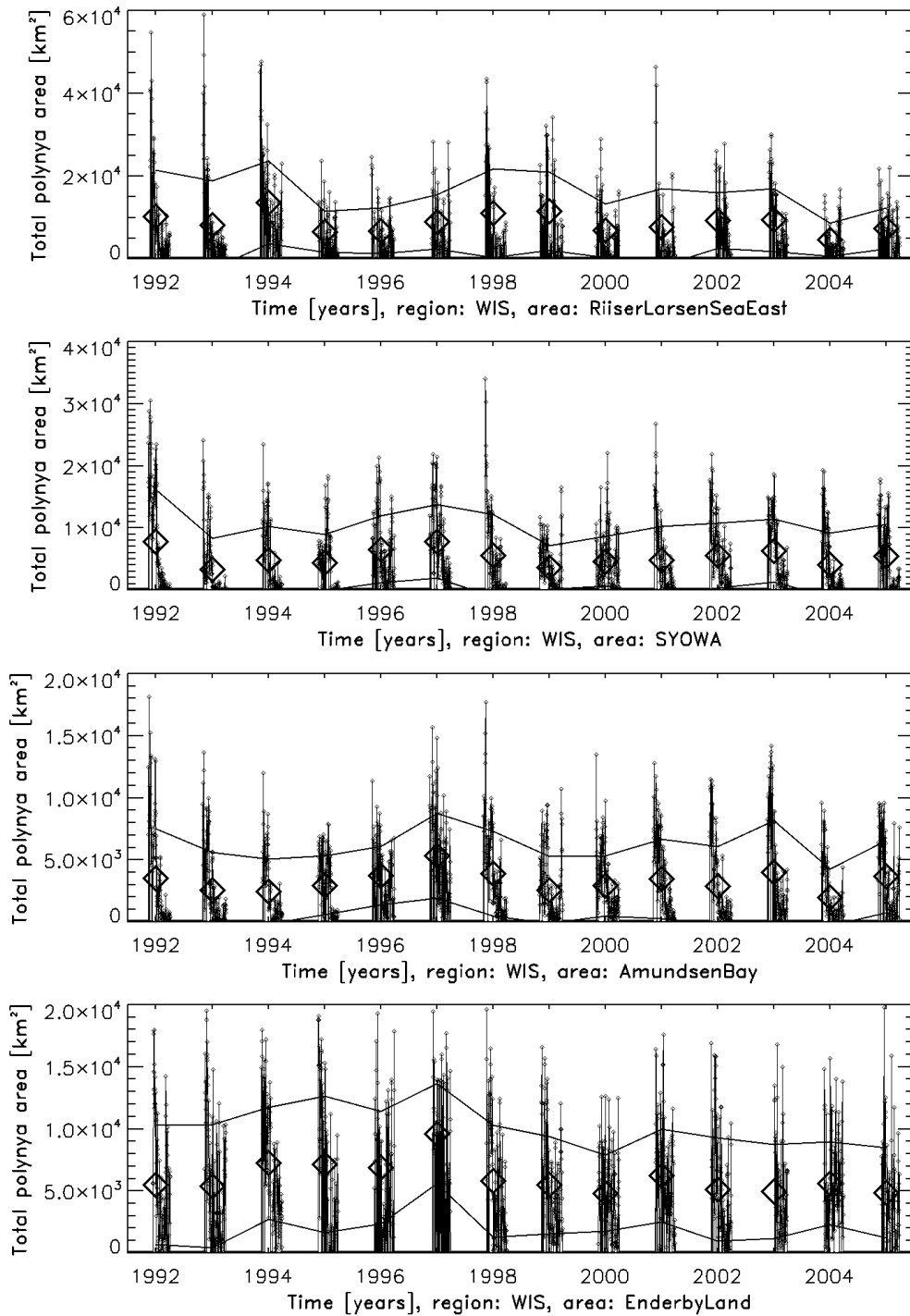


**Figure 32:** Relative polynya distribution of region WIS for 1992-2005 (see caption of Figure 23 for details). The arrow marks Lützow-Holm Bay, the ellipse is referenced in the text.

remained that close to the coast that it has influenced the PSSM analysis even later in the winter. In the remaining years the high polynya probability off Enderby Land (sub-region 4) is most likely associated with the above-mentioned embayments in the ice cover of the Cosmonaut Sea, which eventually form a polynya off the coast. Most pronounced events of this manner took place in 2000 and 2003 as well as in 1992 and 1993.

By comparing Figure 31 with Figure 32 it is evident that the influence of sea ice edge retreat and advance inside region WIS should be rather small for the calculation of the mean total polynya area of sub-regions 1 and 2 – at least after May/June. There might be more influence of this for sub-region 3. Sub-region 4 is certainly influenced by ice edge retreat and advance most often. This sub-region also captures a bit of the Cosmonaut Sea Polynya (when present). This might be of importance when deriving the ice and salt production (Section 9) because this polynya tends to be initiated and maintained, at least partly, by upwelling of warmer

water masses (e.g. Arbetter et al., 2004), which renders this polynya to be of a mixed type, i.e. a latent and sensible heat polynya.



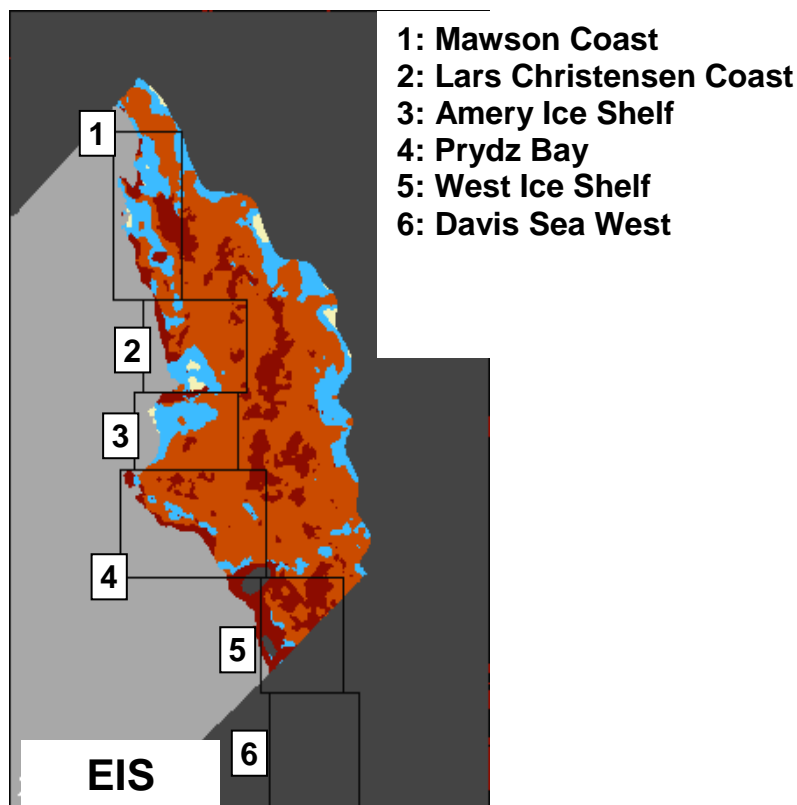
**Figure 33:** Total polynya area of sub-regions 1-4 of region WIS (see Figure 31) for May-Sep. 1992-2005 (see caption of Figure 24 for further details).

Figure 33 summarizes the time series of the (sub-)daily total polynya area of each of the four sub-regions together with the average total polynya area for May.-Sep. for the period 1992-2005. Table 2 lists the displayed average values together with the June-Aug. average and respective standard deviations. The obtained mean total polynya areas take values of around 10 000 km<sup>2</sup>, 5000 km<sup>2</sup>, 3000 km<sup>2</sup>, and 6000 km<sup>2</sup> for sub-regions 1, 2, 3, and 4, respectively. These values decrease substantially (see Table 2), when restricting the analysis to the months

of June to August and thereby reducing the influence of rapid ice edge position changes and/or a still lacking ice cover. The seesaw like structure of the total polynya area as taken from single PSSM maps (see Figure 33, e.g. Amundsen Bay, years: 1992, 1993, 1998, 2001, 2002) indicates, that particularly during May and particularly in sub-region 3 such a restriction is meaningful and that care has to be taken when interpreting the shown time series. For the region east of Lützow-Holm Bay the largest total polynya area occurred 1997.

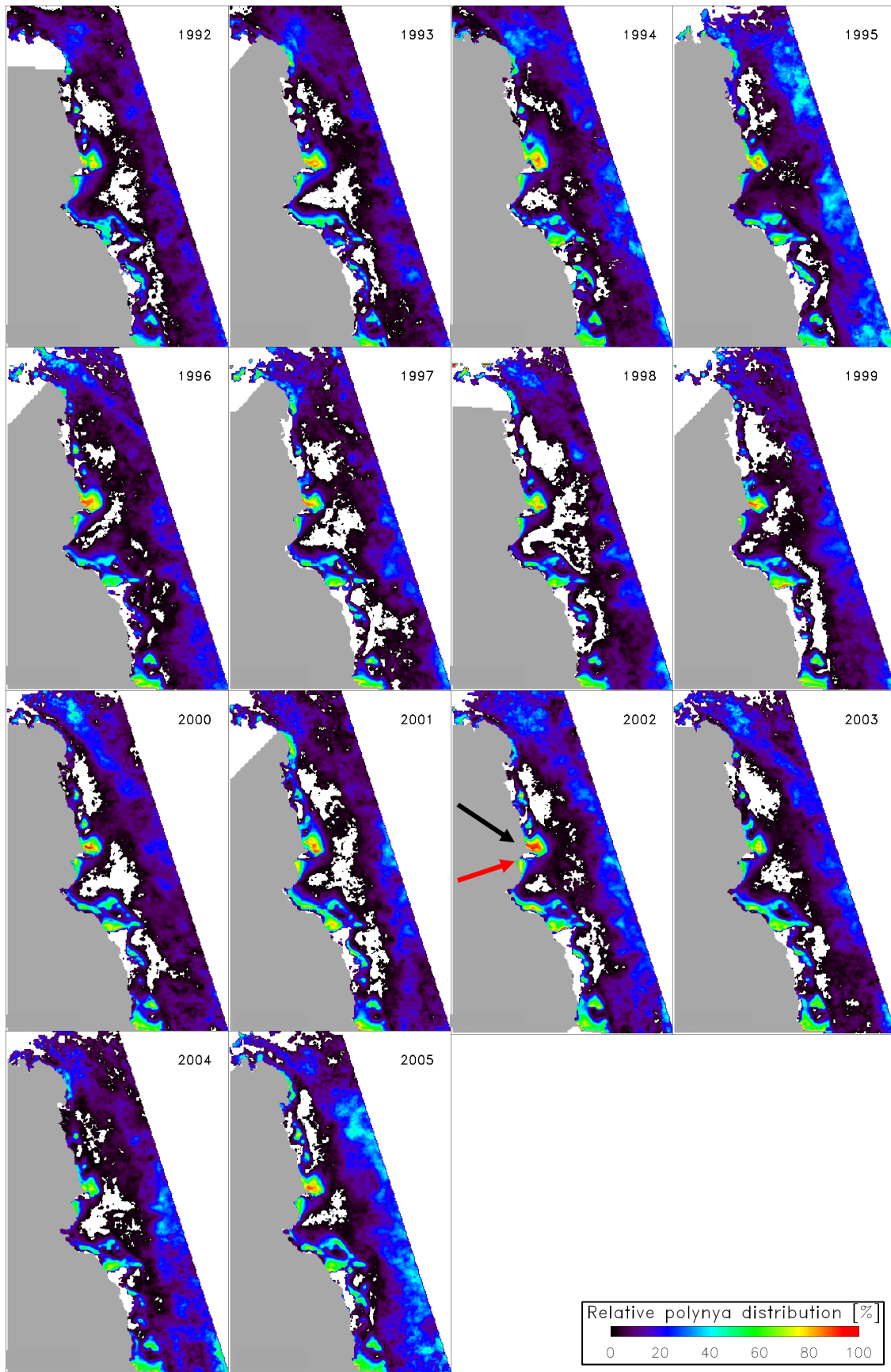
## 8.5 Polynya area: Eastern Indian Ocean Sector (EIS)

Figure 34 shows a sample map of the polynya distribution of region EIS together with the six sub-regions selected of which sub-region 1 overlaps with sub-region 4 of region WIS. Of particular interest in this region are sub-regions 2, 3, and 4; sub-region 2 borders to the East the Cape Darnley, which was recently suggested to be the site of a quite persistent polynya (Tamura et al., 2007, 2008). Sub-regions 3 and 4 border the Amery Ice Shelf and cover Prydz Bay, respectively, areas, which are also known already as sites of enhanced polynya activity (Flocco, 2007). Sub-region 1 borders Mawson Coast, 5 the West Ice Shelf and 6 is located just west of the Shackleton Ice Shelf, covering the southern Davis Sea. All sub-regions except 3 and 5 are beneath a quite steep topography. It can therefore be expected that these sub-regions are subject to quite strong catabatic air flows.



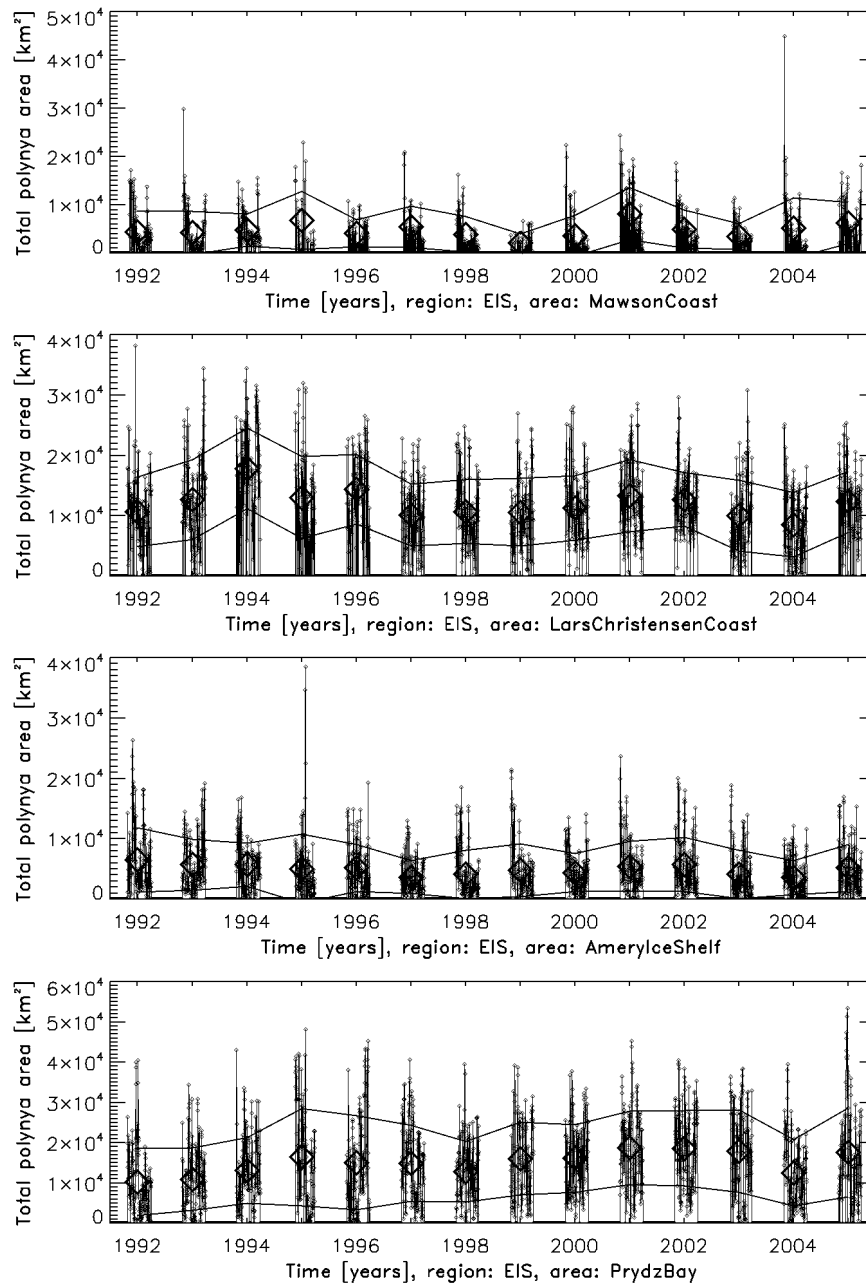
**Figure 34:** Zoom of region EIS – similar to Figure 22.

Figure 35 gives an overview about the relative polynya distribution (polynya probability) for the entire region EIS for May-Sep. for the period 1992-2005. These images reveal two regimes, one regime extending along the coast with areas of high and almost zero polynya probabilities and one further off the coast with a relatively uniform relative polynya distribution between about 20 and 40 %. The latter regime represents the area influenced by



**Figure 35:** Relative polynya distribution of region EIS for the period 1992-2005 (see caption of Figure 23 for details). The black (red) arrow denotes the location of the Cape Darnley (Amery Ice Shelf) Polynya.

ice edge advance and retreat and simply illustrates the variability of the thin ice / open water cover along the ice edge / in the marginal ice zone (MIZ). The first regime is the one of interest concerning the coastal polynyas. These images reveal that sub-regions 1 and 5 can be neglected compared to the other sub-regions in terms of the area within which elevated polynya probabilities are observed with which peak values in the other sub-regions.



**Figure 36:** Total polynya area of sub-regions 1-4 of region EIS (see Figure 34) for May-Sep. 1992-2005 (see caption of Figure 24 for further details).

Polynya probabilities peak a values of 80 %, 80 %, 70% and 95 % in sub-regions Davis Sea, Prydz Bay, Amery Ice Shelf and Lars-Christensen Coast (Cape Darnley polynya, see black arrow in Figure 35), respectively. In particular during winters 1996 and 2002 this last polynya was very persistent and also quite large. An interesting feature is the well-defined narrow area of reduced or almost zero polynya probability between the Cape Darnley Polynya and the Amery Ice Shelf polynya (red arrow in Figure 35), which is evident every year.

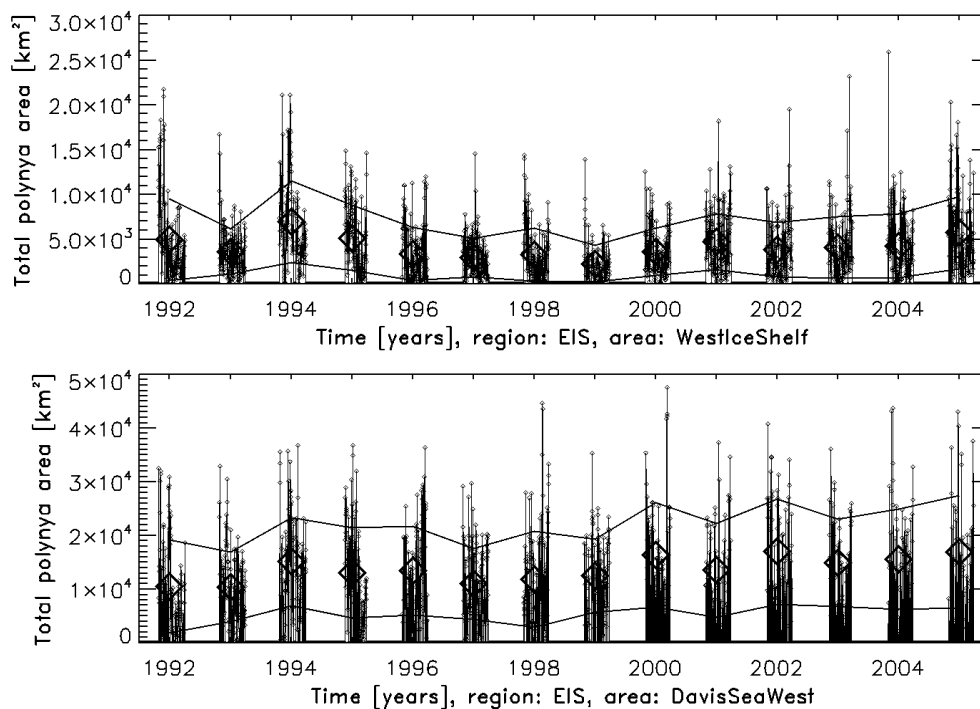


**Figure 36: continued.**

Figure 36 summarizes the time series of the (sub-)daily total polynya area of each of the six sub-regions together with the average total polynya area for May.-Sep. for the period 1992-2005. Table 2 lists the displayed average values together with the June-Aug. average and respective standard deviations.

Figure 36 reveals that sub-regions 2, 4, and 6 (Cape Darnley Polynya, Prydz Bay, and Davis Sea West) contain the largest average total polynya area with values around 10 000 km<sup>2</sup>, ranging from a low of 9000 km<sup>2</sup> to a high of 20 000 km<sup>2</sup>. This compares well with values published by Massom et al (1998). The shown average May-Sep. values for Prydz Bay and Davis Sea West tend to increase, a fact, which can also be observed when restricting the calculation of the mean total polynya area to the months June to August (not shown). Note that in contrast to the region WIS an influence of a retreating / advancing ice edge on the mean total polynya area of the sub-regions of region EIS can be excluded.

## 8.6 Polynya area: Western Pacific Ocean Sector (WPS)

Figure 37 shows a sample map of the polynya distribution of region WPS together with the eight sub-regions selected. Sub-region 1 overlaps with sub-region 6 of region EIS. All sub-regions except sub-region 2 (Shackleton Ice Shelf) are characterized by a coastline with a quite steep topography and (if present) rather narrow ice shelves and are therefore subject to moderate to strong catabatic airflow.

Figure 38 gives an overview about the relative polynya distribution (polynya probability) for the entire region WPS for May-Sep. for the period 1992-2005. As has been shown already for the region EIS (Figure 35), these images reveal two regimes; one regime extends along the coast with areas of high and almost zero polynya probabilities and the other extends further off the coast. The relative polynya distribution is not as uniform as has been shown for the region EIS in this outer regime, and ranges between about 20 and 60 % (in isolated areas 80 %). Still, this regime represents the area influenced by ice edge advance and retreat and simply illustrates the variability of the thin ice / open water cover along the ice edge / in the

MIZ. Since the ice edge is closer to the coastline in the eastern half of region WPS compared to region EIS (as can be deduced from maps showing the monthly mean Antarctic sea-ice extent), the larger contribution of thin ice / open water in the MIZ to the polynya distribution is not surprising. And obviously major changes in the ice edge position occur on the scale of a few days – and are thus not filtered out completely (compare Section 2). However, the sub-regions have been selected such that the contribution of thin ice in the MIZ to the calculation of the total polynya area of the respective sub-region should be negligible.

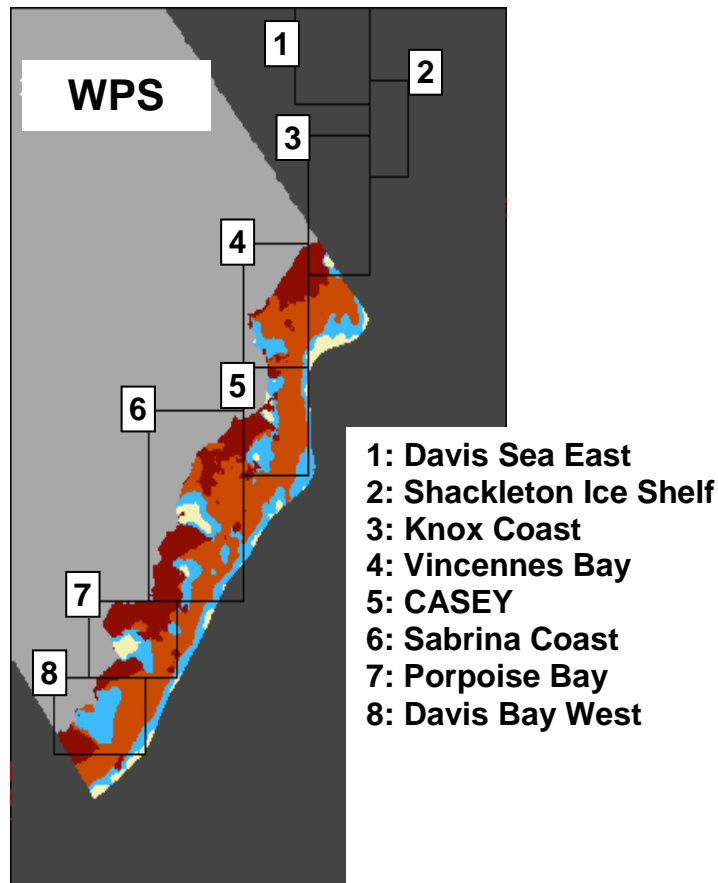


**Figure 37:** Zoom of region WPS – similar to Figure 22.

So again the first regime is the one of interest concerning the coastal polynyas. Sub-regions 4, 5, 6, and 8 (and of course sub-region 1, see text dealing with region EIS) contain the polynyas, which exhibit the highest probability over a considerable area. Within these sub-regions the relative polynya distributions peak mostly at values between 60 and 75 %. The highest probability is observed for sub-region 8, the Davis Bay Polynya. This polynya reveals a high inter-annual variability (compare images for 2004 and 2005 in Figure 38). The Porpoise Bay sub-region (7) also contains a quite well developed polynya; however this is not the case in every year (compare images for 1996-1999 in Figure 38).

Since this region is particularly large compared to the other regions (Figure 2) and, in addition, is subject to a substantial weather influence due to the proximity of the ice edge to the coast, it turned out to be rather difficult to find an appropriate mask to get rid of fast-ice and/or shelf ice that has been misclassified as thin ice (see Section 2). However, a comparison with two recently published fast-ice distribution maps obtained from RADARSAT-1 SAR imagery of November 1997 and 1999 along the East Antarctic coast (Giles et al., 2008) reveals that the mentioned post-processing gives reasonable results. The red and orange circles in Figure 38 mark the area around the Dalton and Dibble Ice Tongues, respectively. Giles et al. (2008) found an about 100 km wide fast-ice coverage to the East of these tongues.